crystals

MDPI

Article

A New Type of White Nephrite from Limestone Replacement along the Kunlun–Altyn Tagh Mountains: A Case from the Mida Deposit, Qiemo County, Xinjiang, China

Tianlong Jiang [1], Guanghai Shi [1,*], Danning Ye [2], Xiaochong Zhang [3], Linjing Zhang [1] and Hongwei Han [4]

[1] State Key Laboratory of Geological Processes and Mineral Resources, China University of Geosciences, Beijing 100083, China; jtlmrright@qlu.edu.cn (T.J.); 2009210024@email.cugb.edu.cn (L.Z.)
[2] National Gems & Jewelry Testing Group Training Center, Shanghai Branch, Shanghai 200021, China; yedanning@126.com
[3] School of Management, Tianjin University of Commerce, Tianjin 300134, China; chong@tjcu.edu.cn
[4] Urumqi Silk Road Deyuan Mining Co., Ltd., Urumqi 830004, China; hanhonwe@163.com
* Correspondence: shigh@cugb.edu.cn

Abstract: The recently discovered Mida nephrite deposit, located in the East Kunlun Mountains, Qiemo County, Xinjiang, Northwest China, contains new types of white and greenish white nephrite formed by limestone replacement, which shows microstructures, macroscopic features and country rocks typologies that are quite different from those of the other deposits along the Kunlun–Altyn Tagh Mountains. The gemological and mineralogical characteristics of Mida nephrite are presented here. These nephrites show an ivory white color and a porcelain-like appearance, with semitranslucent-to-opaque transparency and a porcelain-to-greasy luster. Petrographic study, electron probe microanalysis (EPMA) data and scanning electron microscopy (SEM) images have indicated that the nephrite is composed of tremolite, accompanied by minor quartz, calcite and diopside. Tremolite aggregates have shown different textures, like flaky, granular, fibrous–felted, bundle, radial and metasomatic relict textures. Quartz has appeared in granular or disseminated form, dispersed in the tremolite matrix. Calcite has shown a metasomatic relict texture in the white nephrite samples. Diopside has shown euhedral grains, with some distributed with a certain geometric appearance. Based on our observations, it is suggested that the quartz in the nephrite originated from Si-rich hydrothermal fluids. We propose that the substantial size difference of mineral grains, together with uncompacted grains with inter-particle pores, are the main reasons for the internal reflection and refraction under transmitted light, which allow less transmitted light to pass through the nephrite body and generate the appearance of a semitranslucent-to-opaque transparency, ivory white color and porcelain luster. Our study has unveiled that the Mida nephrite is not typical of the two known types (D-type: dolomite-related; S-type: serpentinite-related) and is overlapped by quartz grains dispersed throughout the less compact tremolite matrix. These observations would help set it apart from the majority of nephrite jades found in the Kunlun Mountains region and provide valuable insights for enhancing comprehension of the diversity of the nephrite deposits.

Keywords: Mida nephrite; quartz; ivory white color; porcelain-like appearance; limestone

Citation: Jiang, T.; Shi, G.; Ye, D.; Zhang, X.; Zhang, L.; Han, H. A New Type of White Nephrite from Limestone Replacement along the Kunlun–Altyn Tagh Mountains: A Case from the Mida Deposit, Qiemo County, Xinjiang, China. *Crystals* **2023**, *13*, 1677. https://doi.org/10.3390/cryst13121677

Academic Editors: Xiaoyan Yu, Fei Liu, Cun Zhang and Sergey V. Krivovichev

Received: 8 November 2023
Revised: 3 December 2023
Accepted: 5 December 2023
Published: 12 December 2023

1. Introduction

Nephrite is a beautiful jade composed mainly of microcrystalline amphibole of the tremolite–actinolite series [1], along with several secondary minerals, such as carbonate minerals, the epidote group, the chlorite group, quartz, rutile, other amphibole minerals, pyrite, and others [2–7]. Nephrite deposits are widespread all over the world and are mainly located in China in the regions of Xinjiang, Guangxi, Qinghai, Liaoning, Guizhou and Taiwan [8–15]. In the other parts of the world, nephrite is found in Russia [16–20],

South Korea [1,21], Australia [1], Canada [22], the United States [1], New Zealand [23,24], Somaliland [25], Afghanistan [26], Vietnam [1], Italy [27], Pakistan [28] and Poland [29].

Based on variations in mineral content and composition, as well as differences in granular morphology and structure, nephrite can exhibit a wide range of colors, transparencies and lusters. White, green, yellow, gray, brown and black nephrites can be found with greasy, waxy or vitreous lusters and fine-to-coarse consistencies [2,6,30]. Tremolites in nephrite usually show distinctive features in terms of grain size, morphology and structure, resulting in notable macroscopic variations. Based on the grain size of the tremolite, nephrite can be divided into three main types: coarse-grained crystalline, microcrystalline and cryptocrystalline [31]. Furthermore, the internal morphological structure of nephrites can be further classified into various types based on the different morphologies and compact textures of the tremolite grains. These include but are not limited to the felt-like, leaf-like, bladed, fibrous, fibrous–cryptocrystalline and radial microscopic blastic textures. Tremolite in nephrite may exhibit metasomatic relict textures like corona, helicitic, diablastic, ring, harbor and pseudomorphic textures [32–34]. In general, nephrite with fine and evenly sized tremolite grains shows a compact microstructure and a delicate and greasy macroscopic appearance, and these characteristics can be observed in nephrites from the regions of Xinjiang, Qinghai and Liaoning.

A major deposit of white and greenish white nephrites (Mida deposit) was recently discovered in the eastern Kunlun Mountains in the region of Qiemo County in Northwest China. The nephrites here have attracted much attention due to their atypical characteristics. Most Mida nephrites show a typical ivory white color, fine texture, semitranslucent-to-opaque transparency and greasy luster, while a smaller portion shows less transparency than the former and a porcelain-like luster. Mida nephrites show distinctive differences from Xinjiang white nephrite, which is known for its fine-grained texture, semitransparent-to-translucent appearance and greasy luster, as well as Qinghai white nephrite, which shows higher transparency and a vitreous luster. Being aware of the potential significance of understanding the formation of nephrite deposits, field investigation and analyses were conducted on this deposit, with a focus on determining the composition and structural characteristics of its component minerals, its microstructure, its macroscopic appearance, the country rock and the connection between the microstructure and the macroscopic appearance.

2. Geological Setting

The Mida nephrite deposit (GPS position: 37°08′51.94″ N, 85°24′23.55″ E, 4069 m) is located in the East Kunlun Mountains (Figure 1).

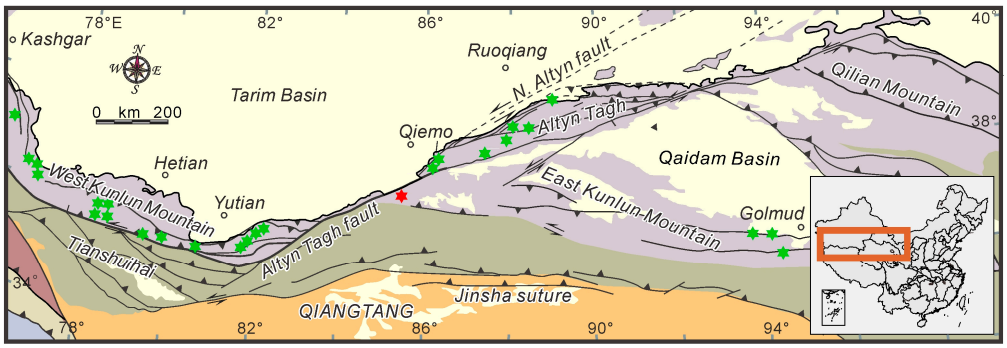

Figure 1. Tectonic map of the northern Tibetan Plateau and the distribution of the primary nephrite deposits in the Kunlun Mountains and Altyn Tagh Mountains (modified after [1,35–38]). Green stars represent the known nephrite deposits, and the red star represents the Mida nephrite deposit.

The Mida nephrite deposit occurs in the Tokuzidaban Formation in Karamiran in the Late Paleozoic trench–arc–basin system between the Altyn fault and Muztag–Jingyu Lake fault (Figure 2). Zircon U–Pb dating of the volcanic rocks in the Tokuzidaban Formation in the Aksu River region indicates the formation age ranges from 364 to 343 Ma [39]. The

Tokuzidaban Formation is located in the South Kunlun terrane, which is part of the East Kunlun Orogenic Belt. The East Kunlun Orogenic Belt is divided into North Kunlun, South Kunlun and Bayan Har terranes based on the boundary between the Central Kunlun fault and the South Kunlun fault [40,41].

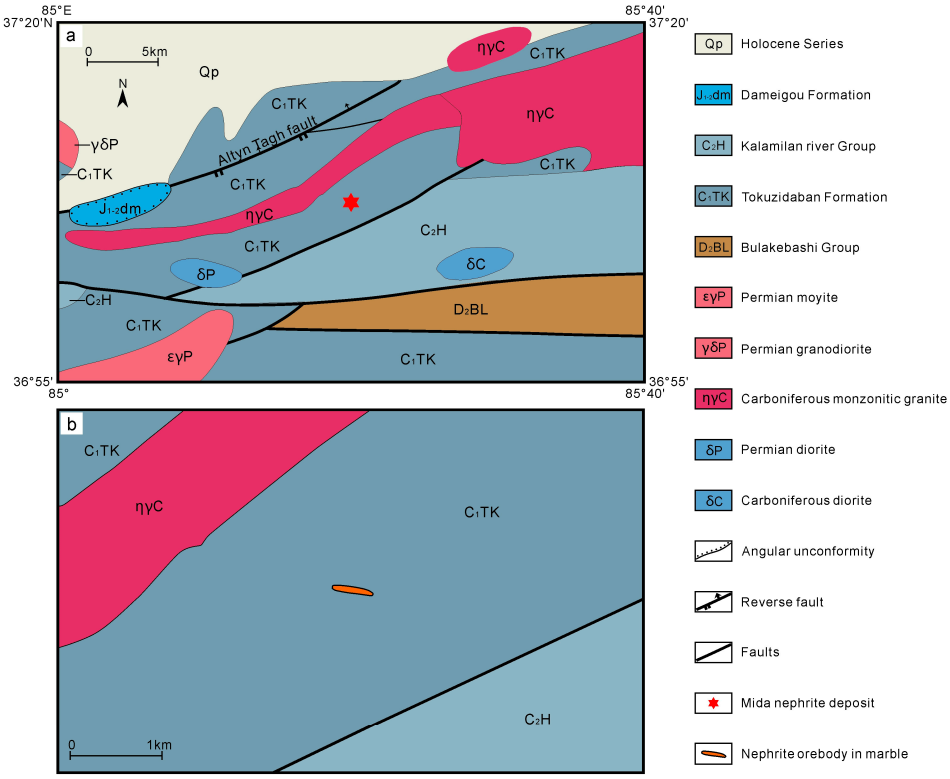

Figure 2. (**a**) Geologic map of the Mida nephrite deposit, modified after National Geological Archives of China (unpublished). (**b**) Nephrite orebody in the Mida nephrite deposit.

Field investigations have revealed that the nephrite orebodies occur as blocks, veins and irregular banded bodies within gray-white or gray-black carbonate rocks composed mainly of marble and marbleized limestone. The main minerals in the carbonate rocks are calcite, with small quantities of tremolite and graphite, along with carbonaceous bands in the center. The carbonate rocks exhibit a large scale, measuring approximately 30 m in horizontal width and over 300 m in length and extending vertically for about 500 m in the Mida nephrite deposit (Figure 3).

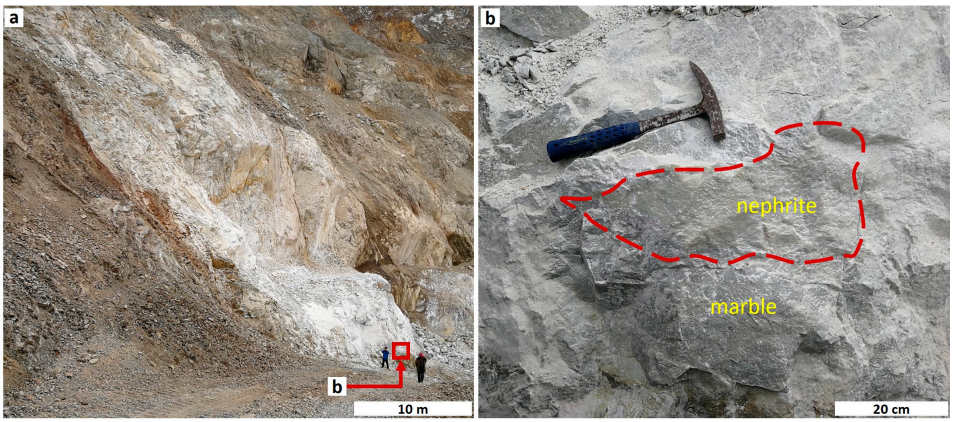

Figure 3. Opencast mining area and orebody of Mida nephrite deposit. (**a**) Outcrop photograph of marbles. (**b**) Nephrite orebody occurs as blocks in gray-black marbles.

The Lower Carboniferous Tokuzidaban Group, mainly composed of limestone, siltstone, silty mudstone and tuff, is found outcropping from the marble. The Tokuzidaban Group consists of sedimentary sea fragments and volcanic fragments with intermediate-basic volcanic rock and partly carbonate rocks. It overlies the Middle Proterozoic strata with a supra-unconformity and has a thickness ranging from 881 to 2788 m. In addition, a high number of fossils occur in the strata of the Tokuzidaban Group, such as coral, brachiopods, bivalves, gastropods, stromatoporoidea, bryozoans, crinoids and microfossils. The monzonitic granite, which is exposed in the northern part of the deposit, intrudes into the Lower Carboniferous Tokuzidaban Group. Additionally, a grey-green vein-like wall can occasionally be observed in close proximity to the nephrite bodies throughout the mining area. During the field investigation, samples of nephrites, wall rocks, marbles and monzonitic granites were collected.

3. Samples and Methods

Among all the samples available to us, we selected four representative nephrites for this study (Figure 4). A small part of the Mida white nephrite exhibits a porcelain-like luster (Figure 4a), while the majority show a typical ivory white color, fine texture, semitranslucent-to-opaque transparency and greasy luster (Figure 4b–d). The color, structure, texture and morphological characteristics of the samples were investigated. Refraction index (RI), specific gravity (SG), Mohs hardness, Fourier transform infrared spectroscopy (FTIR) and powder X-ray diffraction (XRD) were performed at the laboratory of the School of Gemology, China University of Geosciences, Beijing (CUGB). The hardness was examined using a TH763 digital microhardness tester and then converted to Mohs hardness through calculation. We also chose two carbonate rocks for this study (Figure 4e,f). The slices of nephrites and carbonate rocks were observed using an OLYMPUS BX5 polarizing microscope to determine the mineral composition, structural characteristics and contact relationships.

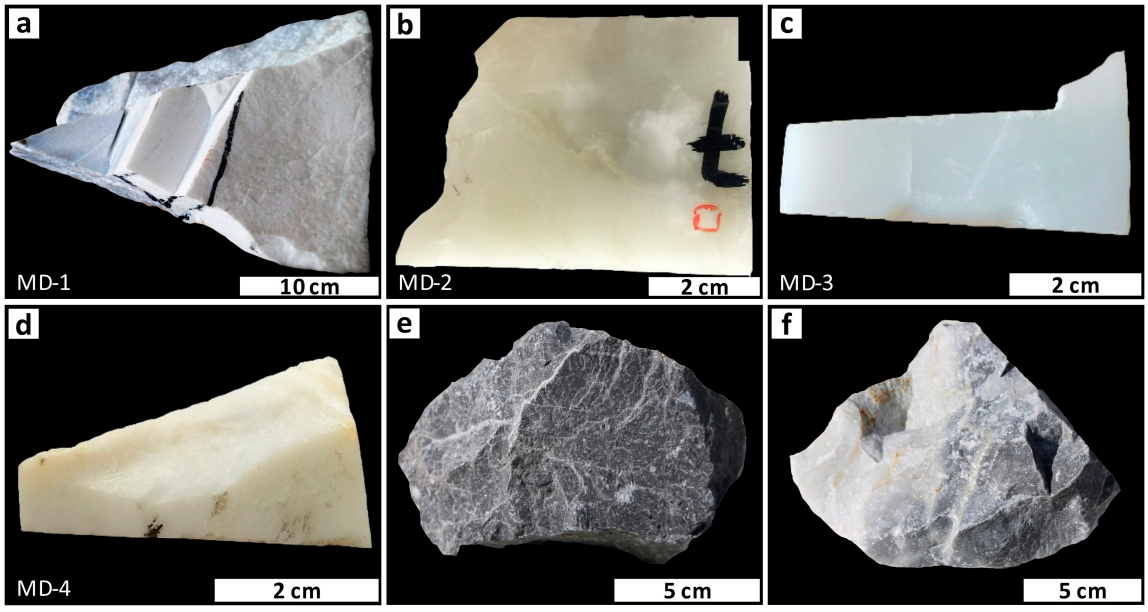

Figure 4. Representative samples of nephrite and carbonate parent rocks from the Mida deposit. (**a**) Representative sample with ivory white color and porcelain-like appearance. (**b**–**d**) Samples with ivory white color and porcelain to greasy luster. (**e**,**f**) Marbleized limestone and marble.

FTIR was performed in reflection mode with a resolution of 4 cm^{-1} over the range of 400–2000 cm^{-1}. A test grating of 6 mm was used, and 32 scans were performed with a Bruker Tensor 27 Fourier transform infrared spectrometer to investigate the main minerals and compare them with Raman spectroscopy results. All samples were crushed and ground

into powders with a size of less than 200 mesh using an agate mortar. The KBr pellets method was employed for analysis. XRD studies were conducted using a Smartlab Rigaku X-ray diffractometer with Cu target, 45 kV–100 mA and scanning speed of 8°/min.

The chemical compositions and backscattered electron (BSE) images of nephrites were acquired using a Shimadzu EPMA–1720 Electron Microprobe Analyzer (EPMA) at the Institute of Earth Sciences, CUGB. The instrument was operated with a 15 kV accelerating voltage, 10 nA beam current and 3 μm spot size. All counting times of element peaks and backgrounds were set to 10 s, with relative sensitivity levels ranging from 0.01 to 0.05 (wt%), an absolute sensitivity of 10^{-14} g, and relative error ranges between 1% and 3%. The instrument was equipped with an X-ray energy spectrometer for qualitative analysis of element contents in the samples to enhance observation efficiency and selection accuracy. Major elements in carbonate rocks were determined through energy-dispersive X-ray fluorescence (EDXRF) using Shimadzu EDX-7000 at the laboratory of the School of Gemology, CUGB.

The surface characteristics and mineral structure of the nephrite were examined using a ZEISS SUPRA 55 scanning electron microscopy (SEM) at the Institute of Earth Sciences, CUGB. The instrument was operated under the following conditions: room temperature of 18 °C, humidity of 30% and acceleration voltage of 15 kV. Each sample was sliced to a size of 1 × 1 cm and coated with carbon powder as a conducting medium.

4. Results

4.1. Gemological Properties

The appearance of the four nephrite jade samples investigated in this paper is similar, and the conventional gemological properties are listed in Table 1.

Table 1. Gemological properties of Mida nephrite.

Scheme	Refractive Index	Specific Gravity	Mohs Hardness
MD–1	1.61	2.86	6.17
MD–2	1.61	2.91	6.42
MD–3	1.62	2.95	6.42
MD–4	1.62	2.90	6.20

All samples are white to grayish white in color. The refraction index ranges from 1.61 to 1.62, the Mohs hardness ranges from 5.97 to 6.21, and the specific gravity ranges from 2.86 to 2.95. The relatively low values of specific gravity, compared to the theoretical range (2.9 to 3.1 [6]), suggest that there may be some minor minerals with lower specific gravity values within the samples.

4.2. Petrography

4.2.1. Nephrite

The Mida nephrite consists of tremolite, with minor accessory minerals of quartz, calcite and diopside.

Tremolite

Under the polarizing microscope, at least two types of tremolite grains can be observed (Figure 5). The first type of grains, which are rare, appear as flakes and bundles approximately 200 μm long and 30 μm wide. Most of the edges and the interiors of these grains exhibit a metasomatic corrosion texture. The second type of tremolite grains display randomly oriented micro to cryptocrystalline fibrous–felted textures with intertwined boundaries. This structure is probably the main factor determining the fine and smooth macroscopic appearance of nephrite.

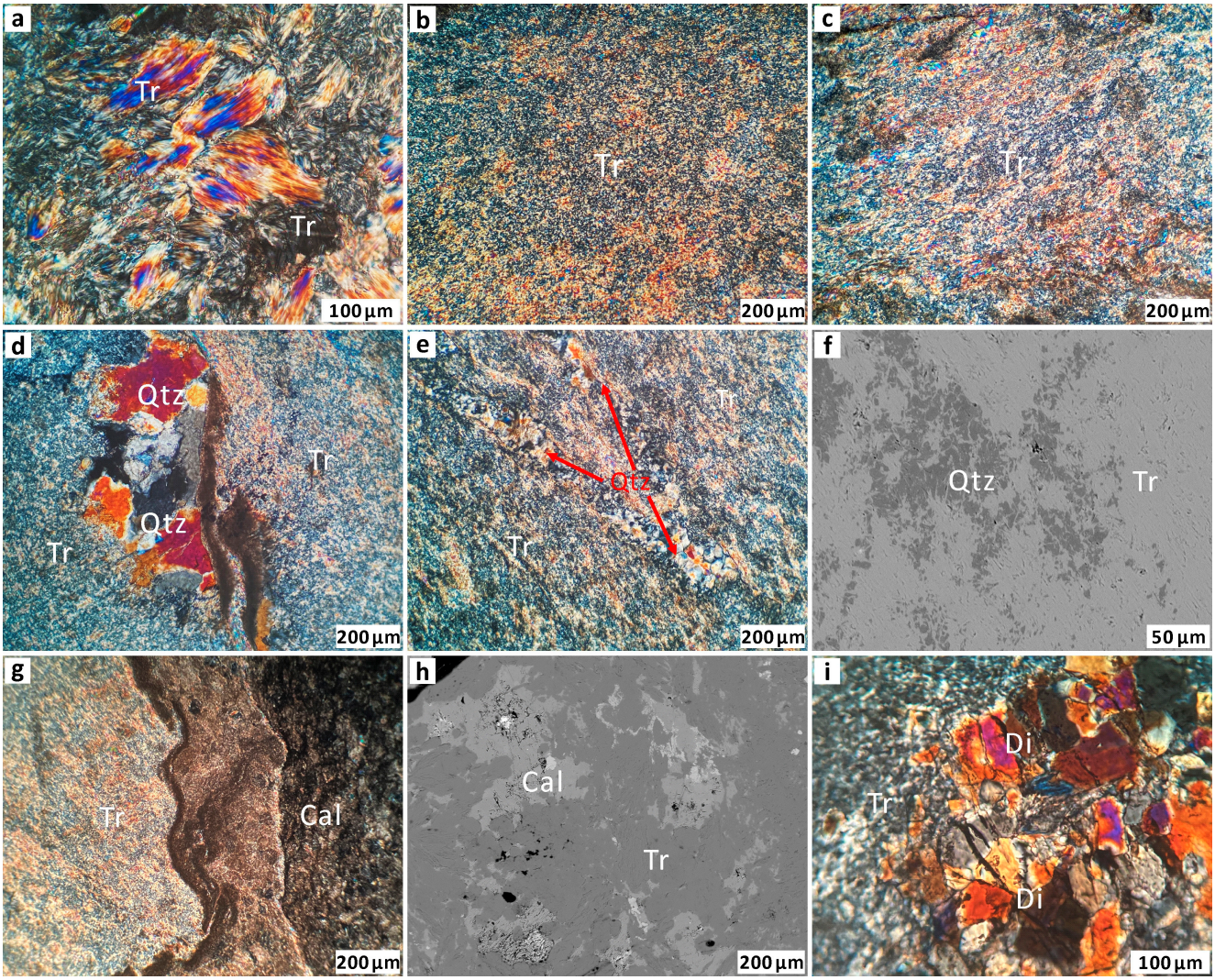

Figure 5. Cross-polarized photomicrographs and BSE images of Mida nephrite. (**a**) Flaky and bundle/fibroblastic texture of tremolite. (**b**) Microscopic felt-like texture of tremolite. (**c**) Fine granular texture of tremolite. (**d**) Granular quartz with metasomatic relict texture in tremolite matrix. (**e**) Quartz vein fill in tremolite matrix. (**f**) BSE image of multiple fine quartz grains dispersed in tremolite matrix. (**g**) Metasomatic contact zone of tremolite and calcite. (**h**) BSE image of relict calcite in tremolite. (**i**) Granular and flaky diopside and granular tremolite grains. Tr—tremolite. Qtz—quartz. Cal—calcite. Di-diopside.

SEM images reveal that the jade domains contain tremolite–actinolite crystals in the form of long, slender fibers measuring approximately 100 µm in length and ranging from 0.1 to 2.0 µm in diameter. Most of these fibers are straight, compacted and oriented parallel or occasionally cross-cutting, while a few exhibit curvature. Additionally, granular and flaky tremolite with interstitial pores can be observed (Figure 6).

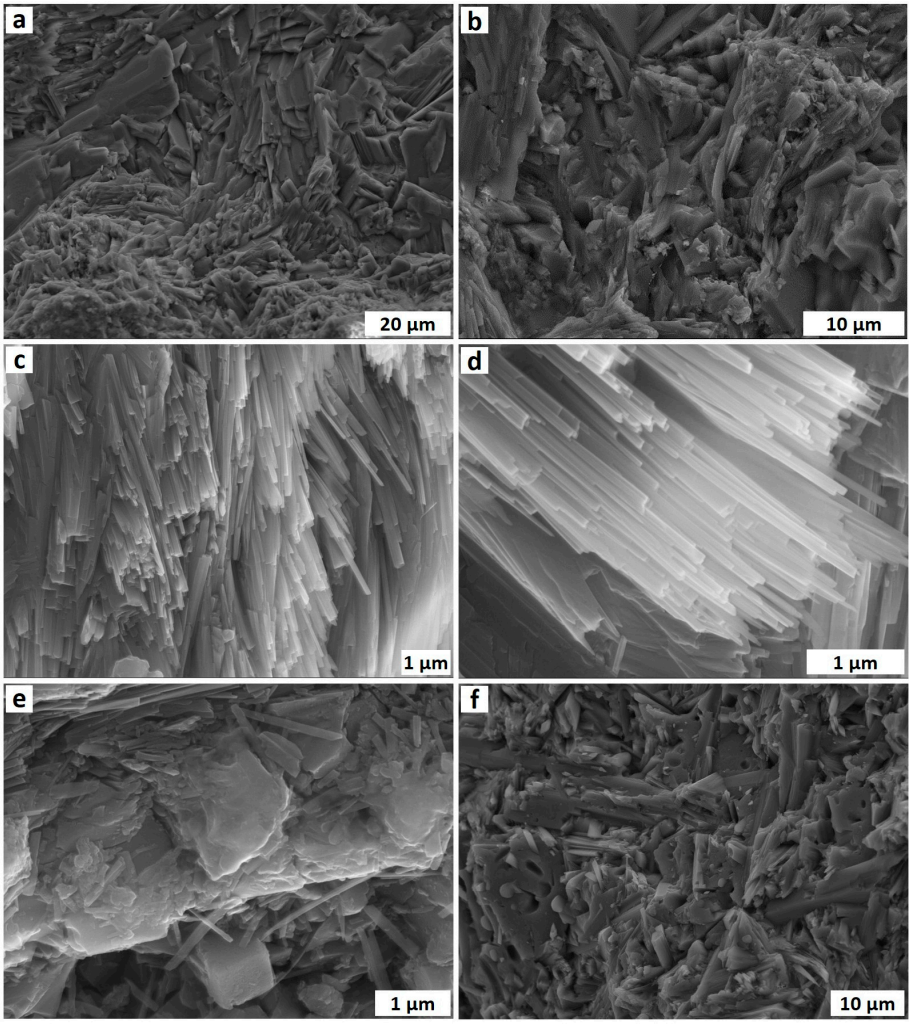

Figure 6. SEM photos of Mida nephrite. (**a**,**b**) Tremolite grains in different sizes. (**c**,**d**) Fine and oriented tremolite bundles. (**e**,**f**) Flaky and granular tremolite grains; pores can be observed between them and on their edges.

Quartz

Based on the shape and stage of formation, quartz grains can be divided into two types (Figure 5). The first type exhibits a metasomatic relict texture, and wave-like extinction is visible under a polarized microscope. The size of quartz grains varies from 1.0 to 400 µm, and they have xenomorphic crystalline shapes. Furthermore, we observe that the granules are dispersed in the tremolite matrix, with their edges being replaced by fibrous tremolite. The second type of quartz occurs as veins that cross-cut through the tremolite matrix.

Calcite

The calcite grains exhibit a granular, crystalloblastic texture with a grain size ranging from 0.2 to 2 mm, and their edges are often replaced by tremolite (Figure 5g,h). Sometimes, irregular calcite veins disseminating in the nephrite can be observed.

Diopside

Granular and flaky diopside grains with a diameter of approximately 50 to 100 µm are observed, occurring alongside fine granular tremolite (Figure 5i).

4.2.2. Carbonate Rocks

The carbonate rocks are mainly composed of marbleized limestone and marble. Among them, the polarizing microscope reveals the presence of biogenic detritus and a micrite matrix (Figure 7). The biogenic detritus primarily consists of Echinodermata, such as fossil crinoid stems and forams.

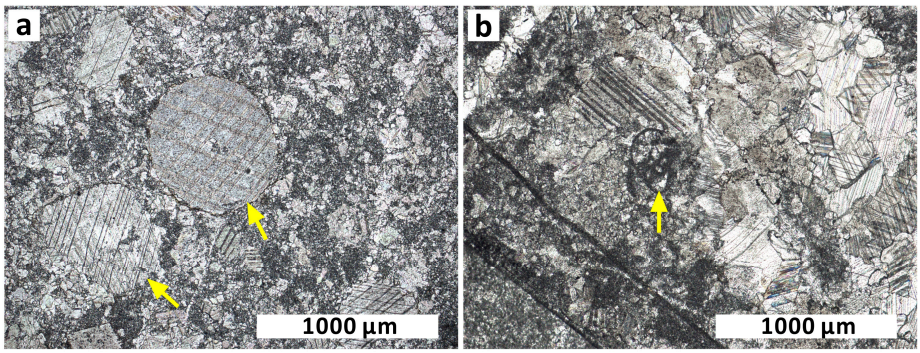

Figure 7. Photomicrographs of the carbonate rocks with biogenic detritus in them. (**a**) Fossil crinoid stems in the carbonate rocks (where the yellow arrows point). (**b**) A fossil foram in the carbonate rocks (where the yellow arrow points).

4.3. Mineral Chemistry

4.3.1. Amphibole

According to the classification diagram based on the chemical composition (Table 2 and Figure 8), the amphiboles belong to the calcic subgroup, which is close to the tremolite end number [42].

Table 2. Chemical composition of tremolite in Mida nephrite (wt%).

Sample	MD–1	MD–2	MD–3	MD–4–1	MD–4–2
SiO_2	59.25	59.04	59.40	59.55	59.13
TiO_2	0.02	0.01	0.01	0.00	0.03
Al_2O_3	0.13	0.29	0.15	0.09	0.11
FeO	0.09	0.17	0.24	0.16	0.09
MnO	0.02	0.38	0.32	0.09	0.08
NiO	0.00	0.03	0.09	0.00	0.06
MgO	24.83	24.10	25.19	24.73	24.77
CaO	13.84	13.18	12.30	13.05	12.71
Na_2O	0.04	0.62	0.09	0.05	0.07
K_2O	0.01	0.21	0.04	0.04	0.08
Total	98.23	98.00	97.84	97.75	97.04
Si	7.98	8.00	8.00	8.00	8.00
Al	0.02	0.00	0.00	0.00	0.00
SumT	8.00	8.00	8.00	8.00	8.00
Al VI	0.00	0.04	0.02	0.01	0.02
Fe^{3+}	0.00	0.00	0.03	0.02	0.00
Mg	4.99	4.87	4.95	4.95	4.98
Fe^{2+}	0.01	0.02	0.00	0.00	0.00
Mn	0.00	0.04	0.00	0.01	0.00
SumC	5.00	4.97	5.00	4.99	5.00
Mg	0.00	0.00	0.11	0.00	0.02
Ni	0.00	0.00	0.01	0.00	0.01
Mn	0.00	0.00	0.04	0.00	0.01
Ca	2.00	1.91	1.78	1.88	1.84
Na	0.00	0.09	0.02	0.01	0.02
SumB	2.00	2.00	1.95	1.89	1.89
Na	0.01	0.07	0.00	0.00	0.00
K	0.00	0.04	0.01	0.01	0.01
SumA	0.01	0.11	0.01	0.01	0.01
$Mg/(Mg+Fe^{2+})$	1.00	1.00	1.00	1.00	1.00
Minerals	**Tr**	**Tr**	**Tr**	**Tr**	**Tr**

Notes: The amphibole formulae were calculated on the basis of 23 oxygens. Tr—tremolite. Fe^{3+} and Fe_2O_3 contents were estimated based on the charge balance [42].

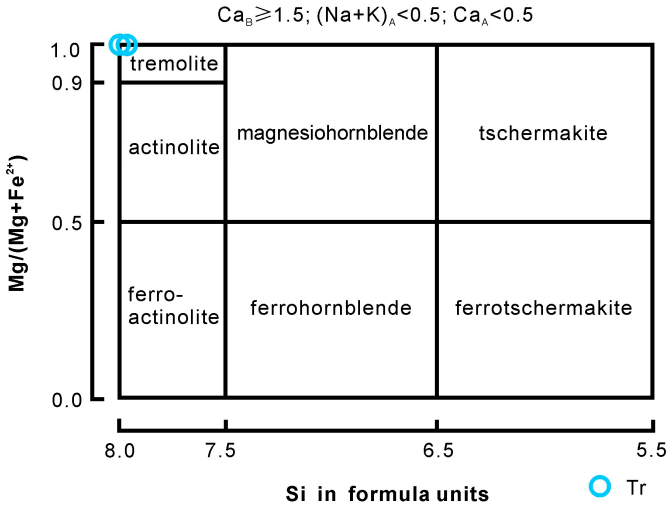

Figure 8. Classification diagram of amphibole in Mida nephrite deposit (after [42]).

4.3.2. Diopside

Diopside in Mida nephrite exhibits a nearly constant chemical composition (Table 3). SiO_2 content ranges from 54.20 to 54.70 wt%, CaO content ranges from 26.12 to 26.46 wt%, and MgO content ranges from 17.69 to 18.48 wt%. FeO content is low, ranging from 0.55 to 0.96 wt%. Based on the general mineral formula ($XY[T_2O_6]$) and sample calculations, the chemical characteristics of diopside are as follows: Si occupies 1.96 to 1.97 atoms per formula unit (a.p.f.u.) on the T site, Mg (M_1) occupies 0.96 to 0.99 a.p.f.u on the Y site, and Ca (M_2) occupies approximately 1.02 a.p.f.u on the X site.

Table 3. Chemical composition of diopside in Mida nephrite (wt%).

Sample	MD–2	MD–3–1	MD–3–2
SiO_2	54.48	54.2	54.7
TiO_2	0.00	0.00	0.05
Al_2O_3	0.01	0.51	0.07
Cr_2O_3	0.03	0.02	0.02
FeO	0.55	0.79	0.96
MnO	0.04	0.02	0.12
MgO	18.48	17.69	18.19
CaO	26.34	26.12	26.46
Na_2O	0.07	0.02	0.01
K_2O	0.00	0.00	0.02
Total	100.01	99.49	100.6
Si	1.96	1.97	1.97
Al	0.00	0.02	0.00
Fe^{3+}	0.02	0.02	0.03
Mg	0.99	0.96	0.98
Ca	1.02	1.02	1.02
Na	0.01	0.00	0.00
Sum	4	3.99	4
Minerals	**Di**	**Di**	**Di**

Notes: The diopside formulae were calculated on the basis of 6 oxygens. Di—diopside. Fe^{3+} and Fe_2O_3 contents were estimated according to the charge balance [42].

4.3.3. Quartz and Calcite

The chemical compositions of quartz and calcite (Table 4) in Mida nephrite indicate that quartz is primarily composed of SiO_2 (98.04–99.44%), while calcite is mainly composed of CaO (56.66–58.13%).

Table 4. Chemical composition of quartz and calcite in Mida nephrite (wt%).

Sample	MD–1	MD–2–1	MD–2–2	MD–4	MD–2	MD–3	MD–4
SiO_2	99.73	99.36	99.80	99.48	0.02	0.06	0.01
TiO_2	0.00	0.04	0.04	0.00	0.00	0.00	0.00
Al_2O_3	0.05	0.02	0.01	0.02	0.01	0.00	0.01
Cr_2O_3	0.01	0.01	0.00	0.00	0.04	0.00	0.00
FeO	0.02	0.00	0.00	0.03	0.04	0.00	0.00
MnO	0.04	0.04	0.01	0.02	0.00	0.00	0.00
NiO	0.00	0.03	0.00	0.00	0.00	0.04	0.00
ZnO	0.00	0.03	0.06	0.03	0.10	0.05	0.00
MgO	0.02	0.29	0.00	0.28	0.00	0.02	0.01
CaO	0.04	0.15	0.03	0.13	56.66	58.13	57.10
Na_2O	0.05	0.02	0.04	0.01	0.03	0.05	0.00
K_2O	0.03	0.01	0.01	0.01	0.00	0.00	0.00
Total	100.00	100.00	100.00	100.00	57.03	58.35	57.19
Minerals	**Qtz**	**Qtz**	**Qtz**	**Qtz**	**Cal**	**Cal**	**Cal**

Notes: Qtz—quartz. Cal—calcite.

4.4. Fourier Transform Infrared Spectroscopy

The infrared ranges of 1200 to 900 cm^{-1} and 600 to 400 cm^{-1} are indicative of the mineral components in Mida nephrite (Figure 9).

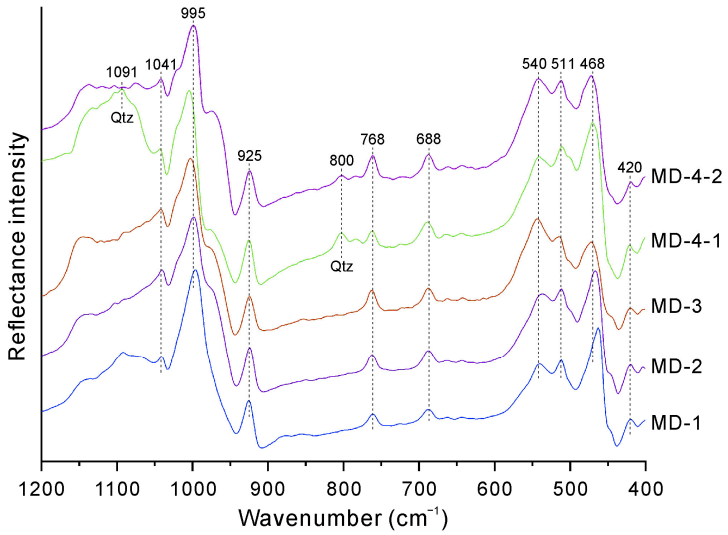

Figure 9. FTIR spectra of the nephrite samples from Mida nephrite deposit.

The vibration absorption peaks observed in all samples at 540 cm^{-1}, 511 cm^{-1}, 468 cm^{-1} and 420 cm^{-1} are attributed to the characteristic Si-O bending vibration, M-O bending vibration and external lattice vibration. Additionally, the peaks at 761 cm^{-1}, 688 cm^{-1}, 663 cm^{-1} and 644 cm^{-1} can be detected in the samples and are assigned to the Si-O-Si symmetric stretching vibration. Furthermore, the peaks at 1136 cm^{-1}, 1041 cm^{-1}, 995 cm^{-1} and 925 cm^{-1} are due to the O-Si-O and Si-O-Si asymmetric stretching vibrations as well as O-Si-O symmetric stretching vibration. Moreover, the presence of other minerals is indicated by certain characteristic vibrational absorption peaks found in some samples, such as diopside (850 cm^{-1} peak), calcite's CO_3^{2-} bending vibration (875 cm^{-1} peak), quartz's Si-O asymmetric stretching vibration (1091 cm^{-1} peak) and quartz's Si-O-Si symmetric vibrations (800 cm^{-1} and 783 cm^{-1} peaks). The band positions and assignments can be found in Table 5.

Table 5. FTIR band assignment of the nephrite samples from Mida nephrite deposit.

Wavenumbers (cm^{-1})	Band Assignment	Suggested Minerals
1136, 1041, 995, 92	O-Si-O and Si-O-Si asymmetric stretching vibration; O-Si-O symmetric stretching vibration	Tr
761, 688, 663, 644	Si-O-Si symmetric stretching vibration	
540, 511, 468, 420	Si-O bending vibration	
1091	Si-O asymmetric stretching vibration	Qtz
800, 783	Si-O-Si symmetric vibration	
875	CO_3^{2-} bending vibration	Cal

Notes: Tr—tremolite. Qtz—quartz. Cal—calcite.

4.5. Powder X-ray Diffraction

The results indicate that Mida white nephrites are relatively pure and mainly composed of tremolite, with minor minerals such as calcite and quartz (Figure 10). The diffraction peaks and their assignment to the identified mineral species are listed in Table 6.

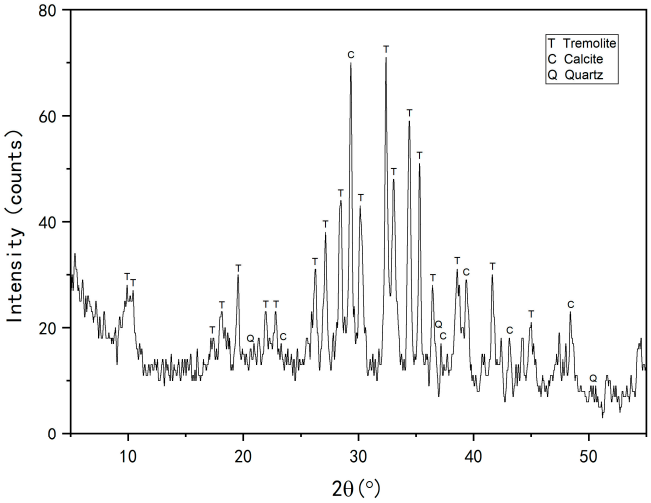

Figure 10. XRD pattern of a sample (MD–3) from Mida nephrite deposit.

Table 6. XRD diffraction peaks and their assignment to the identified mineral species.

2θ (°)	d (Å)	Minerals	2θ (°)	d (Å)	Minerals
9.76	9.0516	Tr	30.36	2.9416	Tr
10.50	8.4183	Tr	32.38	2.7623	Tr
17.36	5.1042	Tr	33.08	2.7058	Tr
18.16	4.8729	Tr	34.50	2.5972	Tr
19.59	4.5275	Tr	35.30	2.5403	Tr
20.85	4.2563	Qtz	36.54	2.4573	Qtz
22.04	4.0218	Tr	38.53	2.3345	Tr
22.81	3.8944	Tr	39.38	2.2865	Cal
23.04	3.8568	Cal	41.71	2.1635	Tr
26.23	3.3947	Tr	43.13	2.0959	Cal
27.18	3.2784	Tr	47.49	1.9131	Cal
28.51	3.1268	Tr	48.44	1.8777	Cal
29.36	3.0391	Cal	50.16	1.8171	Qtz

Notes: Tr—tremolite. Qtz—quartz. Cal—calcite.

4.6. Chemical Characteristics of Carbonate Rocks

The chemical composition of carbonate rocks is listed in Table 7. In all the analyzed samples, the major element contents show limited variations: CaO (52.04–53.44%) and MgO (0.74–1.22%).

Table 7. Chemical composition of carbonate rocks (wt%).

Sample	WY-1-1	WY-1-2	WY-2
SiO_2	0.58	0.53	0.58
Al_2O_3	0.37	0.32	0.36
Fe_2O_3	0.18	0.12	0.19
MnO	0.07	0.04	0.06
NiO	0.04	0.03	0.03
MgO	1.14	0.74	1.22
CaO	52.28	53.44	52.04
K_2O	0.11	0.08	0.11
CuO	0.03	0.03	0.03
SrO	0.03	0.03	0.03
SO_3	0.01	0.01	0.01
SUM	54.83	55.36	54.66

5. Discussion

5.1. Cause of the Ivory White Color and Porcelain-like Appearance of Nephrite

Quartz is present in a granular or disseminated form within the tremolite matrix of a small portion of white Mida nephrite. Samples with a minor amount of quartz exhibit a porcelain-like appearance at a macroscopic level, without any apparent internal features observed under transmitted light. While quartz is mentioned as a minor mineral in many deposits, such as in Utah (USA), Tashisayi and Ruoqiang in Xinjiang (China), Luodian in Guizhou (China), and Sanchakou and Golmud in Qinghai (China) [1,11,41,43,44], the porcelain-like appearance seems to be present only in nephrites with smaller quantities of quartz from the Mida deposit.

The primary factors that determine the light scattering ability are particle size, volume of the second-phase particles and relative refractive index [45]. In all types of jade, the degree of compaction of the granules also influences light penetration because loose parts can be filled with a gas substance having the lowest refractive index. When the grains are uniform in size, well-oriented and tightly interlocking, light can effectively penetrate nephrite, achieving a high level of transparency and exhibiting a greasy to vitreous luster (Figure 11). However, the occurrence of an ivory white color and a porcelain-like appearance in Mida white nephrite may indicate a different internal texture compared to the aforementioned situation. Observations under a polarizing microscope and scanning electron microscope have shown that the white Mida nephrite contains tremolite and quartz grains, with the latter dispersed within the matrix of the former. The size of tremolite grains varies greatly, ranging from 0.05 to 10 μm in width. Similarly, there is significant variability in the size of quartz grains, ranging from 0.05 to 1 mm. A low degree of compaction can also be detected between these grains and their pores.

Consequently, the substantial difference in size between tremolite and quartz grains, along with a low degree of compaction and random orientation of the grains, leads to a reduction in the ability of light to pass through Mida white nephrite (Figure 11c). The significant variation in mineral grain size and random orientation also contribute to an increase in inter-particle pores, the formation of surfaces that are not very smooth and lower internal density. All these factors ultimately cause light to scatter more and consume more energy while passing through some Mida white nephrites. As a result, its ability to reflect surface light and transmit internal light decreases, resulting in a macroscopic appearance characterized by an ivory white color and porcelain texture (Figure 12a). Examples of nephrites corresponding to models a and b are shown in Figure 12b,c.

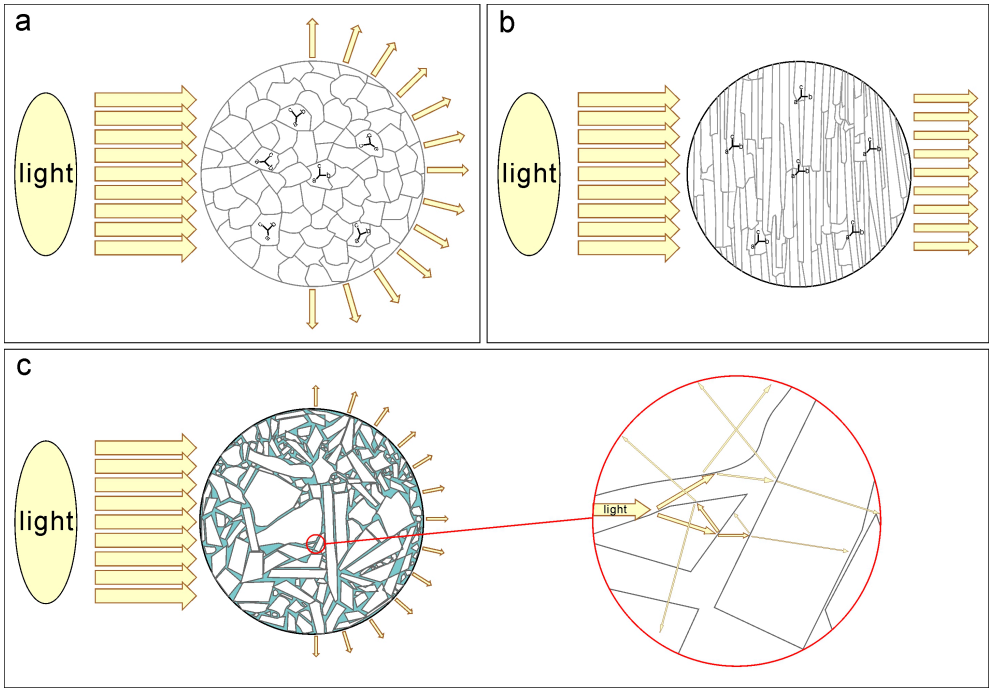

Figure 11. Three models depict light penetrating different textures of the nephrite aggregate. (**a**) The nephrite crystals are fine-grained and compactly intergrown but lack obvious crystallographical orientation. Some transmitted light passes through the nephrite in random directions after internal reflection and refraction, resulting in the typical greasy luster of nephrite. (**b**) The nephrite crystals form a bundle shape with a pronounced crystallographical orientation and are fine-grained. Most of the transmitted light passes through nephrite in a specific direction without significant internal reflection and refraction, creating the vitreous luster and translucent appearance observed in some nephrite from Qinghai province, China. (**c**) In a small portion of Mida nephrite, the grains vary in size and are not fine-grained. Different types and sizes of grains, along with uncompacted texture containing pores, lead to increased internal reflection and refraction, allowing less transmitted light to pass through the nephrite. This generates a semitranslucent-to-opaque transparency as well as a porcelain luster.

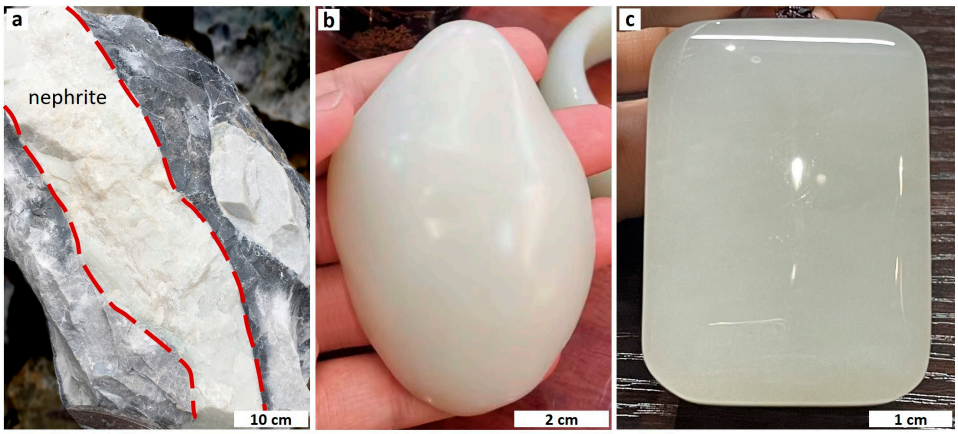

Figure 12. (**a**) A representative hand specimen of Mida white nephrite exhibits an ivory white color and a porcelain luster. (**b**) A polished pendant made from Mida white nephrite showcases fine-grained crystals and a greasy luster. (**c**) A polished pendant made from Qinghai nephrite displays a vitreous luster and a translucent appearance.

5.2. Origin of Quartz in Mida Nephrite

Based on differences in geological background, nephrite deposits can generally be divided into two types: those related to the replacement of dolomite (D-type) and those related to the replacement of serpentinite (S-type) [1,46]. The Mida nephrite deposit is more closely related to the former due to metasomatism between Si-rich hydrothermal fluids and host carbonate rocks. However, it differs from typical D-type nephrites as its occurrence stratum consists of limestone rather than dolomite or dolomitic marble, which distinguishes it from other nephrite deposits along the Kunlun–Altyn Tagh Mountains. The presence of quartz may be connected with this new type of limestone replacement nephrite deposit. However, further study is needed to understand its mechanism.

Although quartz has been mentioned in other nephrite deposits as a minor component, its origin in these deposits and in Mida nephrites has not been extensively investigated. Therefore, determining its origin could be of significant importance. By analyzing the occurrence of quartz in this context, two possible explanations for its presence can be proposed.

The first possibility is that quartz may originate from Si-rich hydrothermal fluids. During the late stage of metasomatism, when the Mg in the ore-forming fluids was nearly depleted, and pressure and temperature values decreased, abundant silica in the hydrothermal fluids began to crystallize as quartz. Crystallization might have occurred within the less compact tremolite matrix, resulting in dispersed quartz grains throughout it.

The second possibility is that quartz may have originated from the host rocks, which are primarily composed of limestone. If the host rocks contained a significant number of quartz particles, they would have participated in reactions during the thermal effect and led to the formation of tremolite. This hypothesis would rely on the evidence of a substantial quantity of quartz grains in the host rocks. However, our observations on the host rock did not confirm this hypothesis.

Therefore, the occurrence of quartz in Mida white nephrites is more likely due to the first hypothesis, suggesting that quartz grains overlapped the less compact tremolite matrix during the formation of the Mida white nephrites. This hypothesis illuminates the potential processes that lead to the formation of nephrites.

6. Conclusions

The gemological and mineralogical characteristics of a white nephrite from the newly discovered Mida deposit are presented. The nephrite exhibits an ivory white color and a porcelain-like appearance with semitranslucent-to-opaque transparency and a porcelain-to-greasy luster. It is mainly composed of tremolite, with minor amounts of quartz, diopside and calcite. Quartz was found in petrographic observation, electron probe microanalysis, Fourier transform infrared spectroscopy and powder X-ray diffraction. Quartz grains were found dispersed in the tremolite matrix, and these observations may be correlated with the appearance of an ivory white color and a porcelain-like appearance rather than the traditional greasy luster.

After investigating the grain size and inter-particle pores, we hypothesize that the difference in size between tremolite and quartz grains, along with low compaction and random grain orientation, is related to the ivory white color and porcelain-like appearance. The occurrence of quartz in nephrite is relatively rare, which could provide valuable insights into the ore-forming process, making it a focal point for further investigation of the Mida nephrite deposit.

Author Contributions: Conceptualization, T.J. and G.S.; methodology, T.J. and G.S.; software, T.J. and D.Y.; validation, T.J. and G.S.; formal analysis, T.J. and D.Y.; investigation, T.J., G.S. and H.H.; resources, T.J. and G.S.; data curation, T.J. and G.S.; writing—original draft preparation, T.J. and G.S.; writing—review and editing, T.J., G.S., X.Z. and L.Z.; visualization, T.J.; supervision, G.S.; project administration, G.S.; funding acquisition, G.S. All authors have read and agreed to the published version of the manuscript.

Funding: This research was funded by the National Key R&D Program of China (Grant No. 2022YFC2903302), the Second Tibetan Plateau Scientific Expedition and Research Program (STHP) (Grant No. 2019QZKK0802) and the National Science Foundation of China (Grant No. 42273044).

Data Availability Statement: The data presented in this study are available in this article.

Acknowledgments: We gratefully appreciate X.H. Lv (Xingfada Inc.), B.Y. Zhang (Xingfada Inc.), S.Q. Wang, and S.C. Wang for their kind support during the field investigation, Z. Yang and X.M. Zhang for help with the preparation of hand specimens and EPMA test, Z.F. Wang for the valuable suggestions, Y.Y. Zhu for the support with image processing, and Y. Li for the support with the photos of the products. The constructive and thoughtful comments and suggestions from X.Y. Yu and four anonymous reviewers, along with editorial handling by Editors are gratefully appreciated.

Conflicts of Interest: Author Hongwei Han was employed by the company Urumqi Silk Road Deyuan Mining Co., Ltd.. The remaining authors declare that the research was conducted in the absence of any commercial or financial relationships that could be construed as a potential conflict of interest. The authors declare no conflict of interest.

References

1. Harlow, G.E.; Sorensen, S.S. Jade (nephrite and jadeitite) and serpentinite: Metasomatic connections. *Int. Geol. Rev.* **2005**, *47*, 113–146. [CrossRef]
2. Lu, L.; Bian, Z.; Wang, F.; Wei, J.; Ran, X. Comparative Study on Mineral Components, Microstructures and Appearance Characteristics of Nephrite from Different Origins. *J. Gems Gemol.* **2014**, *16*, 56–64. (In Chinese with English abstract).
3. Zhou, Z.; Feng, J. A petrological and mineralogical comparison between Xinjiang nephrite and Xiuyan nephrite. *Acta Petrol. Mineral.* **2010**, *29*, 331–340. (In Chinese with English abstract).
4. Prokhor, S.A. The Genesis of Nephrite and Emplacement of The Nephrite–bearing Ultramafic Complexes of East Sayan. *Int. Geol. Rev.* **1991**, *33*, 290–300. [CrossRef]
5. Tang, Y.; Liu, D. Geological characteristics of Manasi green jade in Xinjiang. *Acta Petrol. Mineral.* **2002**, *21*, 22–25. (In Chinese with English abstract).
6. Wang, S. *A Book of Gem–Jade Resources in China*; Scientific and Technical Documentation Press: Beijing, China, 1999; pp. 15–20.
7. Ling, X.; Schmadicke, E.; Li, Q.; Gose, J.; Wu, R.; Wang, S.; Liu, Y.; Tang, G.; Li, X. Age determination of nephrite by in-situ SIMS U–Pb dating syngenetic titanite: A case study of the nephrite deposit from Luanchuan, Henan, China. *Lithos* **2015**, *220–223*, 289–299. [CrossRef]
8. Jing, Y.; Liu, Y. Genesis and mineralogical studies of zircons in the Alamas, Yurungkash and Karakash Rivers nephrite deposits, Western Kunlun, Xinjiang, China. *Ore Geol. Rev.* **2022**, *149*, 105087. [CrossRef]
9. Shi, M.; Yu, B.; Guo, Y.; Yuan, Y.; Ng, Y. Structural and Mineralogical Characterization of Green Nephrite in Hetian, Xinjiang, China. *Key Eng. Mater.* **2014**, *633*, 159–164. [CrossRef]
10. Yin, Z.; Jiang, C.; Santosh, M.; Chen, Y.; Bao, Y.; Chen, Q. Nephrite Jade from Guangxi Province, China. *Gems Gemol.* **2014**, *50*, 228–235. [CrossRef]
11. Yu, H.; Wang, R.; Guo, J.; Li, J.; Yang, X. Study of the minerogenetic mechanism and origin of Qinghai nephrite from Golmud, Qinghai, Northwest China. *Sci. China Earth Sci.* **2016**, *59*, 1597–1609. [CrossRef]
12. Qiu, Z.; Jiang, Q.; Han, L.; Qin, S.; Li, L. Raman Spectra and Its Application of Graphite Enclaves in Nephrite–Jades in Xiuyan, Liaoning. *Spectrosc. Spectr. Anal.* **2010**, *30*, 2985–2988. [CrossRef]
13. Gao, S.; Bai, F.; Heide, G. Mineralogy, geochemistry, and petrogenesis of nephrite from Tieli, China. *Ore Geol. Rev.* **2019**, *107*, 155–171. [CrossRef]
14. Li, N.; Bai, F.; Xu, L.; Che, Y. Geochemical characteristics and ore–forming mechanism of Luodian nephrite deposit, Southwest China and comparison with other nephrite deposits in Asia. *Ore Geol. Rev.* **2023**, *160*, 105604. [CrossRef]
15. Yui, T.; Usuki, T.; Chen, C.; Ishida, A.; Sano, Y.; Suga, K.; Iizuka, Y.; Chen, C. Dating thin zircon rims by NanoSIMS: The Fengtien nephrite (Taiwan) is the youngest jade on Earth. *Int. Geol. Rev.* **2014**, *56*, 1932–1944. [CrossRef]
16. Kislov, E.V.; Popov, M.P.; Nurmukhametov, F.M.; Posokhov, V.F.; Vanteev, V.V. Nyrdvomenshor Nephrite Deposit, Polar Urals, Russia. *Minerals* **2023**, *13*, 767. [CrossRef]
17. Kislov, E.V.; Erokhin, Y.V.; Popov, M.P.; Nikolayev, A.G. Nephrite of Bazhenovskoye Chrysotile–Asbestos Deposit, Middle Urals: Localization, Mineral Composition and Color. *Minerals* **2021**, *11*, 1227. [CrossRef]
18. Khudyakova, L.I.; Kislov, E.V.; Paleev, P.L.; Kotova, I.Y. Nephrite–Bearing Mining Waste as a Promising Mineral Additive in the Production of New Cement Types. *Minerals* **2020**, *10*, 394. [CrossRef]
19. Burtseva, M.; Ripp, G.; Posokhov, V.; Zyablitsev, Y.; Murzintseva, A. The sources of fluids for the formation of nephritic rocks of the southern folded belt of the Siberian Craton. *Geochemistry* **2015**, *460*, 82–86. [CrossRef]
20. Burtseva, M.V.; Ripp, G.S.; Posokhov, V.F.; Murzintseva, A.E. Nephrites of East Siberia: Geochemical features and problems of genesis. *Russ. Geol. Geophys.* **2015**, *56*, 402–410. [CrossRef]
21. Yui, T. Origin of a Dolomite–Related Jade Deposit at Chuncheon, Korea. *Econ. Geol.* **2002**, *97*, 593–601. [CrossRef]

22. Leaming, S.F. *Jade in Canada*; Geological Survey of Canada: Ottawa, ON, Canada, 1978; pp. 2–50.
23. Adams, C.J.; Beck, R.J.; Campbell, H.J. Characterisation and origin of New Zealand nephrite jade using its strontium isotopic signature. *Lithos* **2007**, *97*, 307–322. [CrossRef]
24. Cooper, A.F. Nephrite and Metagabbro in the Haast Schist at Muddy Creek, Northwest Otago, New Zealand. *New Zealand J. Geol. Geophys.* **1995**, *38*, 325–332. [CrossRef]
25. Shi, G.; Jia, R.; Santosh, M.; Liang, H.; He, H. First report of a nephrite deposit from Somaliland, Africa: Characterization and geological and archaeological implications. *Geol. Soc. Am. Bull.* **2023**. [CrossRef]
26. Obiadi, S.S.; Amini, M.A.; Fazli, F. Mineralogy and Geochemistry of Nephrite from Wolay Deposite, Kunar, East Afghanistan. *J. Mech. Civ. Ind. Eng.* **2022**, *3*, 56–65. [CrossRef]
27. Adamo, I.; Bocchio, R. Nephrite jade from Val Malenco, Sondrio, Italy: Review and new data. *Gems Gemol.* **2013**, *49*, 98–106. [CrossRef]
28. Umar, Z.; Liaqat, U.; Ahmed, R.; Baig, M. Classification of Nephrite Using Calibration–Free Laser Induced Breakdown Spectroscopy (CF–LIBS) with Comparison to Laser Ablation–Time-of-Flight–Mass Spectrometry (LA–TOF–MS). *Anal. Lett.* **2020**, *53*, 203–216. [CrossRef]
29. Gil, G.; Bagiński, B.; Gunia, P.; Madej, S.; Sachanbiński, M.; Jokubauskas, P.; Belka, Z. Comparative Fe and Sr isotope study of nephrite deposits hosted in dolomitic marbles and serpentinites from the Sudetes, SW Poland: Implications for Fe–As–Au–bearing skarn formation and post–obduction evolution of the oceanic lithosphere. *Ore Geol. Rev.* **2020**, *118*, 103335. [CrossRef]
30. Suo, L.; Tao, Z.; Yuan, Z. Mineral composition and chemical composition of Chinese nephrite. *Miner. Resour. Geol.* **2019**, *33*, 484–488. (In Chinese with English abstract).
31. Tang, Y.; Chen, B.; Jiang, R. *Chinese Hetian Nephrite*; Xinjiang People's Publishing House: Urumqi, China, 1994; pp. 100–205.
32. Wu, R.; Li, W.; Ao, Y. Research on Texture and Structure Type of Hetian Jade in Xinjiang. *J. Gems Gemol.* **1999**, *1*, 7–10. (In Chinese with English abstract).
33. Wang, S.; Duan, T.; Zheng, Z. Mineralogical and petrological characteristics of Xiuyan nephrite and its minerogenetic model. *Acta Petrol. Mineral.* **2002**, *21*, 79–90. (In Chinese with English abstract).
34. Liu, F.; Yu, X.Y. Classification and mineralogical characteristics of nephrite deposits in China. *Miner. Resour. Geol.* **2009**, *23*, 375–380. (In Chinese with English abstract).
35. Zhang, X.; Shi, G.; Zhang, X.; Gao, K. Formation of the Nephrite Deposit with Five Mineral Assemblage Zones in the Central Western Kunlun Mountains, China. *J. Petrol.* **2022**, *63*, egac117. [CrossRef]
36. Xiong, F.; Ma, C.; Zhang, J.; Liu, B.; Jiang, H. Reworking of old continental lithosphere: An important crustal evolution mechanism in orogenic belts, as evidenced by Triassic I–type granitoids in the East Kunlun orogen, Northern Tibetan Plateau. *J. Geol. Soc.* **2014**, *171*, 847–863. [CrossRef]
37. Cowgill, E.; Yin, A.; Harrison, T.M. Reconstruction of the Altyn Tagh fault based on U–Pb geochronology: Role of back thrusts, mantle sutures, and heterogeneous crustal strength in forming the Tibetan Plateau. *J. Geophys. Res.* **2003**, *108*, 2346. [CrossRef]
38. Xiao, W.; Windley, B.F.; Yong, Y.; Yan, Z.; Yuan, C.; Liu, C.; Li, J. Early Paleozoic to Devonian multiple–accretionary model for the Qilian Shan, NW China. *J. Asian Earth Sci.* **2009**, *35*, 323–333. [CrossRef]
39. Xu, X.; Liu, C.; Liu, W.; Ye, B.; Zhao, Z.; Ma, B. Geochronology and geochemistry of the Late Devonian–Early Carboniferous volcanic rocks in Aksu River area, western end of the East Kunlun Orogen. *Geol. J.* **2020**, *55*, 2881–2901. [CrossRef]
40. Zhou, S. Palaeogeography of the Carboniferous in Xinjiang. *Xinjiang Geol.* **2000**, *18*, 324–329. (In Chinese with English abstract).
41. Xu, Z.; Li, H.; Yang, J. An orogenic plateau–the orogenic collage and orogenic types of the Qinghai Tibet plateau. *Earth Sci. Front.* **2006**, *13*, 1–17. (In Chinese with English abstract).
42. Leake, B.E.; Woolley, A.R.; Arps, C.E.S.; Birch, W.D.; Gilbert, M.C.; Grice, J.D.; Hawthorne, F.C.; Kato, A.; Kisch, H.J.; Krivovichev, V.G.; et al. Nomenclature of amphiboles: Report of the subcommittee on amphiboles of the International Mineralogical Association, Commission on New Minerals and Mineral Names. *Can. Mineral.* **1997**, *35*, 219–246. [CrossRef]
43. Jiang, Y.; Shi, G.; Xu, L.; Li, X. Mineralogy and Geochemistry of Nephrite Jade from Yinggelike Deposit, Altyn Tagh (Xinjiang, NW China). *Minerals* **2020**, *10*, 418. [CrossRef]
44. Zhi, Y.; Liao, G.; Chen, Q.; Li, Y.; Zhou, Z. The discovery of the Luodian nephrite in Guizhou Province and its petrological and mineralogical characteristics. *Acta Petrol. Mineral.* **2011**, *30*, 58–62. (In Chinese with English abstract).
45. Kingery, W.D.; Bowen, H.K.; Uhlmann, D.R. *Introduction to Ceramics*; Wiley–Interscience: New York, NY, USA, 1976; pp. 20–82.
46. Nichol, D. Two contrasting nephrite jade types. *J. Gemol.* **2000**, *4*, 193–200. [CrossRef]